

Characteristics of yttrium oxide laser ceramics with additives

V.V. Osipov, V.I. Solomonov, A.N. Orlov, V.A. Shitov, R.N. Maksimov, A.V. Spirina

Abstract. Neodymium- or ytterbium-doped laser ceramics with a disordered crystal-field structure formed by introduction of iso- and heterovalent elements into yttrium oxide are studied. It is shown that these additives broaden the spectral band of laser transitions, which makes it possible to use ceramics as active laser media emitting ultrashort pulses. Lasing was obtained in several samples of this ceramics. At the same time, it is shown that addition of zirconium and hafnium stimulates the Förster quenching of upper laser levels and pump levels.

Keywords: ceramics, laser oscillation, yttrium oxide, zirconium, hafnium, Förster quenching.

1. Introduction

The possibility of creating highly transparent Y_2O_3 ceramics by introducing ThO_2 as a densifying additive was demonstrated for the first time by the General Electric Company (USA) [1]. This material, which was called Yttralox, contains 10 mol % of ThO_2 and 90 mol % of Y_2O_3 , and its optical transmission in the visible region is close to that of glass. In [1], it was also shown that ZrO_2 or HfO_2 can be used as additives as well. The authors of [2] believe that thorium dioxide forms thorium solid solution in the near-boundary regions of crystallites in yttrium oxide, which decreases the surface energy and mobility of boundaries and thus decreases the amount of pores.

In [3–5], it was reported on the creation of a technology of production of highly transparent Y_2O_3 ceramics with addition of 10 mol % of ThO_2 and 1 mol % of Nd_2O_3 . The best quality of this ceramics, sufficiently high for obtaining laser oscillation, was achieved when this ceramics was rapidly cooled after sintering. This procedure reduced the formation of submicron scattering centres, which led to a decrease in optical losses.

The authors of [6–11] developed a technology of highly transparent Y_2O_3 ceramics with additions of ZrO_2 and HfO_2 . In contrast to ThO_2 , these additives are radiation safe, but they also allow one to achieve a high transparency of ceram-

ics. In particular, the transparency of yttrium oxide ceramics at a wavelength of 6 μm was as high as 86% in the case of addition of 10 mol % of HfO_2 and 82% with addition of 10 mol % of ZrO_2 . The introduction of these additives with concentrations higher than 15 mol % leads to the appearance of inter-crystallite porosity and to a decrease in the ceramics density, which deteriorates its optical properties. The same authors also showed that the introduction of 15–30 mol % of Sc_2O_3 to yttrium oxide causes deformation of the crystal lattice and appearance of vacancies of both signs, because of which the sintering of ceramics occurs much faster. Later, these investigations were continued in order to create laser ceramics [12–15]. The concentrations of ZrO_2 and HfO_2 additives in such ceramics are much smaller. In particular, in [13, 14], it was clearly shown that the optimal concentration of ZrO_2 is ~ 3 mol %, which is probably related to a difference in powders or in the introduction methods.

It should be noted that, in all the mentioned works, ThO_2 , Sc_2O_3 , ZrO_2 , and HfO_2 were introduced as sintering additives to improve the ceramics quality due to increasing its density and transparency.

For the first time, the introduction of additives in order to obtain a disordered crystal structure of ceramic grains and, hence, a broader gain band of dopant ions was studied in [16]. The authors of this work synthesised $Nd^{3+}:Y_3ScAl_4O_{12}$ ceramics in which the gain bandwidth of Nd^{3+} ions reached 5.5 nm, which allowed them to achieve laser pulses with a duration of 10 ps. The gain bandwidth of ytterbium ions in $Yb^{3+}:Y_3(Sc_{0.5}Al_{0.5})_5O_{12}$ ceramics in [17] was 12.5 nm, and the laser pulse duration was decreased to 580 fs. The maximum gain bandwidth (30 nm) for the neodymium ion was achieved in disordered $Nd^{3+}:Ba(Zr, Mg, Ta)O_3$ ceramics, which emitted laser pulses with a duration of 1.4 ps [18]. The shortest (112 fs) pulses were achieved in $Yb^{3+}:(Y,Gd)_2Sc_2(GdAl_2)O_{12}$ ceramics [19] with a gain bandwidth of 14.4 nm. It should be noted that the shortest laser pulses (53 fs) have been achieved to date in combined $Yb^{3+}:Sc_2O_3-Yb^{3+}:Y_2O_3$ ceramics with the total gain bandwidth of 27.8 nm [20]. Experiments on increasing the spectral gain bandwidth in $Nd^{3+}:Y_2O_3$ ceramics were continued in [21]. There it was shown that the introduction of 12 mol % of ZrO_2 and 24 mol % of Lu_2O_3 or Sc_2O_3 makes it possible to increase the laser transition bandwidth to 40 nm.

In the present paper, we give the results of the synthesis and characterisation of optical ceramics based on pure yttrium oxide and on yttrium oxide with addition of iso- and heterovalent (Zr^{4+} or Hf^{4+}) ions. As dopants, we used Yb^{3+} or Nd^{3+} ions in amount of ~ 1 at % of the content of trivalent cations.

V.V. Osipov, V.I. Solomonov, A.N. Orlov, V.A. Shitov, R.N. Maksimov, A.V. Spirina Institute of Electrophysics, Ural Branch, Russian Academy of Sciences, ul. Amundsena 106, 620016 Ekaterinburg, Russia; e-mail: plasma@iep.uran.ru

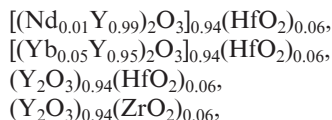
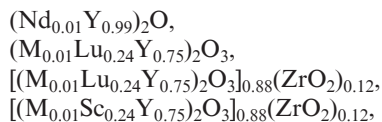
Received 24 October 2012; revision received 25 January 2013

Kvantovaya Elektronika 43 (3) 276–281 (2013)

Translated by M.N. Basieva

2. Investigation objects

Initial materials for producing highly transparent ceramics are nanopowders. The nanopowders were obtained by a laser synthesis method described in detail in [22]. We synthesised nanopowders of solid solutions based on monoclinic yttrium oxide of the following compositions:



where $\text{M} = \text{Yb}^{3+}$ or Nd^{3+} . The concentration of uncontrolled impurities did not exceed 0.001%.

These nanopowders were compacted by a uniaxial static press under a pressure of 133–200 MPa into disks 15 mm in diameter with a thickness of 3–4 mm and a density equal to 0.48–0.51 of the X-ray density. Then, the disks were annealed in air at temperatures of 800–1100 °C to burn off organic residues and transform the solid solution from the monoclinic to the cubic phase. After this, the compacts were sintered in a GERO HTK-8W/22-1G-HV vacuum furnace with tungsten heaters at temperatures of 1700 and 1950 °C during 20 and 10 h, respectively. The X-ray diffraction analysis performed on a D8 Discover diffractometer showed that all the ceramic samples were solid solutions of corresponding additives in cubic yttrium oxide.

3. Results and discussion

Figure 1 shows the photographs of the best samples of synthesised ceramics after annealing and polishing. The microstructure of the samples was studied in detail in [23–27], where the dimensions of crystallites after polishing and chemical etching were determined using an Olympus BX51TRF optical microscope. It was found that the average sizes of crystallites decrease with decreasing sintering temperature and depend on the impurity composition. For example, at a sintering temperature of 1700 °C, the largest average sizes of crystallites

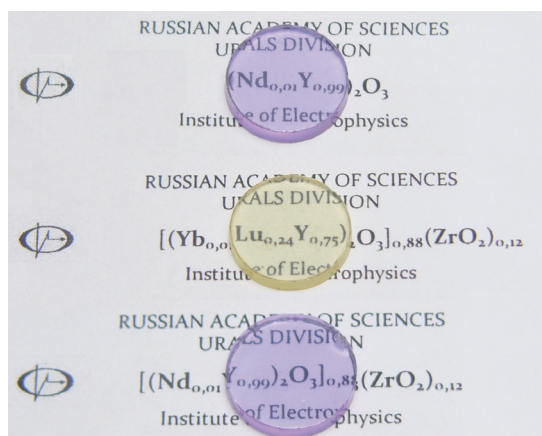


Figure 1. Photographs of the best samples of synthesised ceramics.

(8 μm) were observed in impurity-free $(\text{Nd}_{0.01}\text{Y}_{0.99})_2\text{O}_3$ ceramics. The introduction of 24 mol % of Sc_2O_3 and 12 mol % of ZrO_2 decreased these dimensions to 5 μm, and the substitution of scandium for lutetium decreased the crystallite sizes to 1 μm. At a sintering temperature of 1950 °C, the average sizes of crystallites increased to 60 μm in impurity-free $(\text{Nd}_{0.01}\text{Y}_{0.99})_2\text{O}_3$ ceramics and to 20–25 μm in ceramics with addition of ZrO_2 .

All the samples contained pores with average sizes of 1–3 μm, which were localised mainly on crystallite interfaces. The amount of pores decreased with increasing sintering temperature and with introduction of zirconium. In particular, at the sintering temperature of 1700 °C, the content of pores was 200 ppm in the impurity-free $(\text{Nd}_{0.01}\text{Y}_{0.99})_2\text{O}_3$ sample and 90–130 ppm in the samples with impurities. At the same time, at the sintering temperature of 1950 °C, the content of pores in the $(\text{Nd}_{0.01}\text{Y}_{0.99})_2\text{O}_3$ samples decreased to 13–22 ppm and the samples with addition of ZrO_2 have no pores at all.

We measured the optical characteristics of ceramics, namely, the optical transmission, the luminescence spectrum (including the spectrum in the region of the laser transition), and the lifetime of the upper laser level. As well as in [24–27], the optical transmission of ceramics was measured using a Shimadzu UV-1700 double-beam spectrophotometer. The transmission spectrum did not differ from the spectrum presented in [24–27]. The neodymium-doped samples showed strong absorption lines of the Nd^{3+} ion in the entire studied wavelength range, while the samples doped with ytterbium ions exhibited an absorption band of the Yb^{3+} ion in the region of 880–1010 nm. Addition of ZrO_2 , HfO_2 , Lu_2O_3 , and Sc_2O_3 do not change the transmission spectra of the samples. In the region of the laser wavelength (1.03–1.07 μm), the transparency of the $[(\text{Nd}_{0.01}\text{Y}_{0.99})_2\text{O}_3]_{0.88}(\text{ZrO}_2)_{0.12}$ ceramics (81.4%) turned out to be approximately the same as of the impurity-free $(\text{Nd}_{0.01}\text{Y}_{0.99})_2\text{O}_3$ ceramics (81.3%), while this parameter of the $[(\text{Yb}_{0.01}\text{Lu}_{0.24}\text{Y}_{0.75})_2\text{O}_3]_{0.88}(\text{ZrO}_2)_{0.12}$ sample was 80.6%.

The IR luminescence spectra and the lifetimes of the upper laser level of dopant ions were measured upon excitation of ceramic samples by a laser diode with a power of 3 W at the wavelength $\lambda = 808 \pm 3$ nm for Nd^{3+} and $\lambda = 977 \pm 3$ nm for Yb^{3+} . The optical emission spectrum of the neodymium-doped ceramics contains several lines (Fig. 2) caused by the

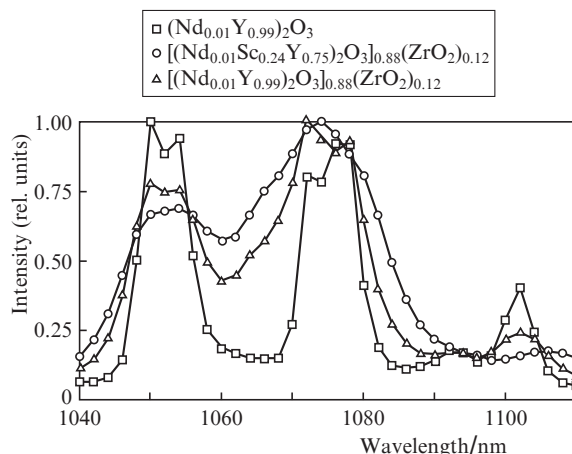


Figure 2. IR luminescence spectra of ceramic samples doped with Nd^{3+} ions.

transitions between the Stark components of the ${}^4F_{3/2}$ and ${}^4I_{11/2}$ levels. With addition of Sc^{3+} and Zr^{4+} , these lines overlap and form one broad emission band. For the $(Nd_{0.01}Y_{0.99})_2O_3$, $[(Nd_{0.01}Y_{0.99})_2O_3]_{0.88}(ZrO_2)_{0.12}$, and $[(Nd_{0.01}Sc_{0.24}Y_{0.75})_2O_3]_{0.88}(ZrO_2)_{0.12}$ samples, the transition line-width at a level of 0.4 of the maximum intensity is 11.4, 36, and 40 nm, respectively.

The IR luminescence spectrum of Yb^{3+} -doped ceramics contains two bands (Fig. 3). Their maxima correspond to the optical transitions from the lower Stark sublevel of the ${}^2F_{5/2}$ state to the third ($\lambda \approx 1030$ nm) and fourth ($\lambda \approx 1075$ nm) Stark sublevels of the ground ${}^2F_{7/2}$ state of the Yb^{3+} ion. It should be noted that the positions of these peaks for ceramics with different additives are noticeably different, which relates to different crystal-field symmetries. However, these bands overlap at intensities of 0.25–0.55 of the maximum for ceramics of different compositions and form one band with a width reaching 85–100 nm at a level of 0.1.

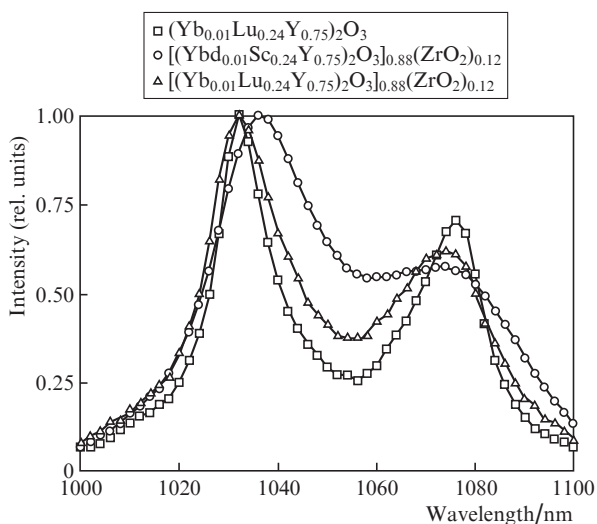


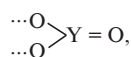
Figure 3. IR luminescence spectra of ceramic samples doped with Yb^{3+} ions.

The lasing properties of the obtained ceramics were studied at the Institute of Laser Physics, Siberian Branch, Russian Academy of Sciences (Novosibirsk, Russia). Lasing in the ceramic samples shown in Fig. 1 was obtained previously, namely, in the $(Nd_{0.01}Y_{0.99})_2O_3$ sample at $\lambda = 1079$ nm with a slope efficiency of 15% and an optical efficiency of 10% [25, 26] and in the sample $[(Yb_{0.01}Lu_{0.24}Y_{0.75})_2O_3]_{0.88}(ZrO_2)_{0.12}$ at $\lambda = 1034$ nm with a slope efficiency of 29% and an optical efficiency of 9.4% [27]. Attempts to obtain lasing in poreless $[(Nd_{0.01}Y_{0.99})_2O_3]_{0.88}(ZrO_2)_{0.12}$ ceramics with the highest optical transmittance (81.4%) were unsuccessful.

To clarify the reason for the relatively low lasing efficiency in the first two samples and its absence in the $[(Nd_{0.01}Y_{0.99})_2O_3]_{0.88}(ZrO_2)_{0.12}$ ceramics, we performed kinetic investigations of the IR luminescence at the optical transitions from the upper laser levels of neodymium and ytterbium ions. The photoluminescence kinetics was recorded by an FD-24K photodiode and a Tektronix TDS520 oscilloscope. The upper laser levels were excited by the same laser diodes as when measuring the photoluminescence spectra.

Previously [24, 27], it was shown that, after switching off the pump pulse with a duration larger than 1000 μs , the

decrease in the intensity of the IR luminescence of neodymium ions at the transitions from the ${}^4F_{3/2}$ level for $(Nd_{0.01}Y_{0.99})_2O_3$ and $[(Nd_{0.01}Y_{0.99})_2O_3]_{0.88}(ZrO_2)_{0.12}$ ceramics is described by a close-to-exponential law with the effective times $\tau_{eff} = 190$ and 180 μs , respectively (the time τ_{eff} corresponds to the intensity decrease by a factor of e). The lifetime of the upper laser level of Nd^{3+} ions in the impurity-free $(Nd_{0.01}Y_{0.99})_2O_3$ ceramics was measured to be 190 μs , which is noticeably shorter than the corresponding lifetime previously measured in analogous single crystals (255 μs) [28] and in similar ceramics [29]. In this case, the role of intrinsic acceptors in the studied ceramic samples can be played by bound radicals



Nd^{3+} ions in distorted lattice sites, surface defects, and discontinuities (dislocations). Additional studies of the IR luminescence kinetics showed that the time τ_{eff} for these ceramics strongly decreases with decreasing pump pulse duration t_{ex} (Fig. 4). The effective time τ_{eff} in the $[(Nd_{0.01}Y_{0.99})_2O_3]_{0.88}(ZrO_2)_{0.12}$ ceramics is by 5%–6% shorter than in the $(Nd_{0.01}Y_{0.99})_2O_3$ ceramics at all excitation durations.

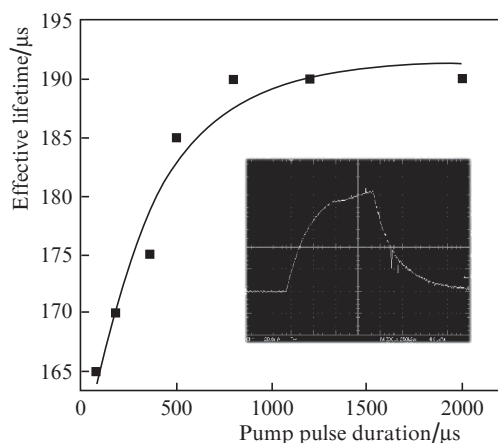


Figure 4. Dependence of the effective lifetime τ_{eff} of the upper laser level on the pump pulse duration in $(Nd_{0.01}Y_{0.99})_2O_3$ ceramics. The inset shows the oscillogram of an IR luminescence pulse at $t_{ex} = 800$ μs ; scan duration is 200 μs .

This behaviour of τ_{eff} indicates that the measured effective times are not the radiative lifetimes τ_r of the ${}^4F_{3/2}$ level of the Nd^{3+} ion, since the latter must not change so strongly in the cubic crystal fields of the studied ceramics. In particular, according to the data of [28], the radiative lifetimes in the Y_2O_3 (cubic symmetry T_h) and $Y_3Al_5O_{12}$ (cubic symmetry O_h^{10}) matrices are close to each other, $\tau_r = 260$ and 255 μs , respectively. Computer approximation of the slope of the IR luminescence intensity in these ceramics showed that, with a correlation coefficient higher than 0.99, the slope is described by an exponential function with the exponent equal to the algebraic sum of the linear and square-root terms,

$$I(t) = I_0 \exp\left(-\frac{t}{\tau_r} - \sqrt{\frac{t}{\tau_F}}\right). \quad (1)$$

Here, I_0 is the initial intensity at the moment of switching off of excitation. Formula 1 coincides with the classical formula

for the Förster luminescence decay at τ_r corresponding to the radiative lifetime of the upper laser level of the neodymium ion and τ_F corresponding to the characteristic time of quenching of this level due to the energy transfer to acceptors. However, we found that, with decreasing pump pulse duration t_{ex} from 1000 to 80 μs at approximately the same radiative time $\tau_r \approx 254 \mu\text{s}$, the time τ_F decreases from 2110 to 1020 μs in the $[(\text{Nd}_{0.01}\text{Y}_{0.99})_2\text{O}_3]_{0.88}(\text{ZrO}_2)_{0.12}$ ceramics and from 3000 to 1300 μs in the $(\text{Nd}_{0.01}\text{Y}_{0.99})_2\text{O}_3$ ceramics. Within the static Förster model, where $\tau_F = (\tau_r/\pi)(C_0/C_a)^2$ (C_a is the acceptor concentration and C_0 is the acceptor concentration at which the probability of energy transfer from a donor to an acceptor is π/τ_r), the observed dependence on t_{ex} can be related to a change in the acceptor concentration C_a formed to the end of the pump pulse. In particular, this situation occurs when the pump pulse excites not only dopant ions but also the centres playing the role of acceptors. As a result, the excited centres lose the acceptor properties. In this case, the concentration of acceptors C_a formed to the end of the pump pulse tends to a minimum value with increasing pump pulse duration.

The Förster quenching occurs due to the dipole–dipole interaction of the luminescent ion (donor) with an acceptor. This interaction has a resonance character due to the overlap of the luminescence band of the donor with the absorption band of the acceptor. This means that the acceptor must have energy levels resonant with the upper laser level $^4\text{F}_{3/2}$ or with the pump level $^4\text{F}_{5/2}$ of the Nd^{3+} ion. The absorption and emission bands of acceptors are masked by the bands of the dopant ion and are difficult to observe in the spectra of doped ceramics.

The transmission spectra of undoped ceramics of pure yttrium oxide, as well as of ceramics with addition of zirconium and hafnium, show two weak absorption bands with the maxima at $\lambda = 821$ and 852 nm overlapping with the absorption bands of the Nd^{3+} ion at the transitions $^4\text{I}_{9/2} \rightarrow ^4\text{F}_{5/2,3/2}$. Obviously, these absorption bands belong to the centres that play the role of acceptors in the impurity-free $(\text{Nd}_{0.01}\text{Y}_{0.99})_2\text{O}_3$ ceramics and are responsible for the quenching of the upper laser levels of the neodymium ion.

The same absorption centres quench the upper laser levels of the neodymium ion in doped ceramics with zirconium and hafnium. However, the time τ_F in these ceramics is smaller than in the impurity-free $(\text{Nd}_{0.01}\text{Y}_{0.99})_2\text{O}_3$ ceramics. This means that ceramics with zirconium and hafnium additives contains additional acceptors. The role of acceptors can be played by the ions of admixtures. The Zr^{4+} and Hf^{4+} ions with closed electronic shells cannot be acceptors, but the trivalent Zr^{3+} and Hf^{3+} ions with the $3\text{d}^{10}4\text{d}^1$ and $4\text{f}^{14}5\text{d}^1$ electronic configurations of the ground states can readily serve as acceptors. In crystals, these configurations form orbital doublet (E) and triplet (T_2) energy levels spaced by $10Dq$ (crystal field strength).

It is obvious that the bands of the Zr^{3+} and Hf^{3+} ions in the transmission and luminescence spectra of ceramics with zirconium and hafnium are difficult to detect due to their overlap with the strong absorption and emission bands of neodymium ions. To illustrate this, Fig. 5a shows the pulsed cathode luminescence (PCL) spectrum of the $[(\text{Nd}_{0.01}\text{Y}_{0.99})_2\text{O}_3]_{0.88}(\text{ZrO}_2)_{0.12}$ ceramics, which in fact consists of two emission bands of the neodymium ion in the transition from the $^4\text{F}_{3/2}$ and $^4\text{F}_{5/2}$ levels to the ground state. The same PCL spectrum is observed for the $[(\text{Nd}_{0.01}\text{Y}_{0.99})_2\text{O}_3]_{0.94}(\text{HfO}_2)_{0.06}$ ceramics.

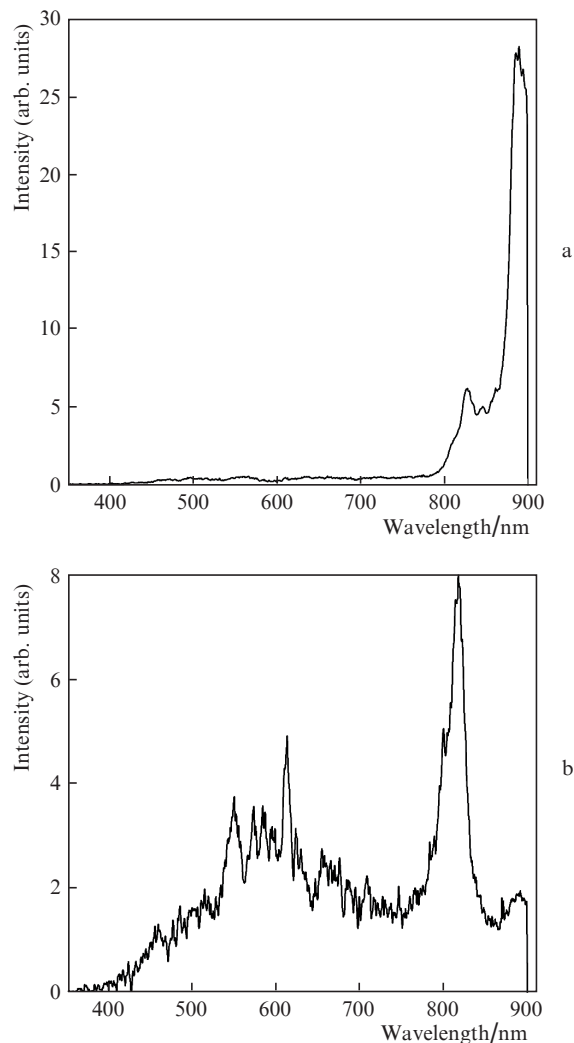
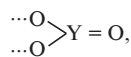


Figure 5. Measured PCL spectra of doped $[(\text{Nd}_{0.01}\text{Y}_{0.99})_2\text{O}_3]_{0.88}(\text{ZrO}_2)_{0.12}$ (a) and $[(\text{Yb}_{0.05}\text{Y}_{0.95})_2\text{O}_3]_{0.94}(\text{HfO}_2)_{0.06}$ (b) ceramics.

However, the PCL spectrum of the same ceramics doped with ytterbium (Fig. 5b) contains, in addition to the well-known luminescence band of Y_2O_3 emitted by the bound radical [30]



a strong band peaking at $\lambda \approx 818 \text{ nm}$ and a band in the region of $\lambda = 900 \text{ nm}$, at the edge of the photodetector spectral range. These bands are typical for undoped ceramics with zirconium and hafnium additives (Fig. 6), but are absent in the PCL spectrum of Y_2O_3 [30]. The new observed luminescence bands with the maxima at $\lambda \approx 818$ and 900 nm can be interpreted as the emission bands of Zr^{3+} (Hf^{3+}) ions in sites with close-to-tetrahedral symmetry, in which the crystal field strength is $11000\text{--}13000 \text{ cm}^{-1}$. These sites can be probably formed in the cubic lattice of yttrium oxide in the case of substituting the main Y^{3+} cation by the quadrivalent Zr^{4+} (Hf^{4+}) ion.

Indeed, in the cubic lattice of yttrium oxide, the yttrium ion lies in the centre of the YO_6 elementary cube, the natural oxygen vacancies lying in cube corners along the face diagonal in $1/3$ of these cubes and along the body diagonal in $2/3$ of these cubes [31]. To compensate the electric charge of zirco-

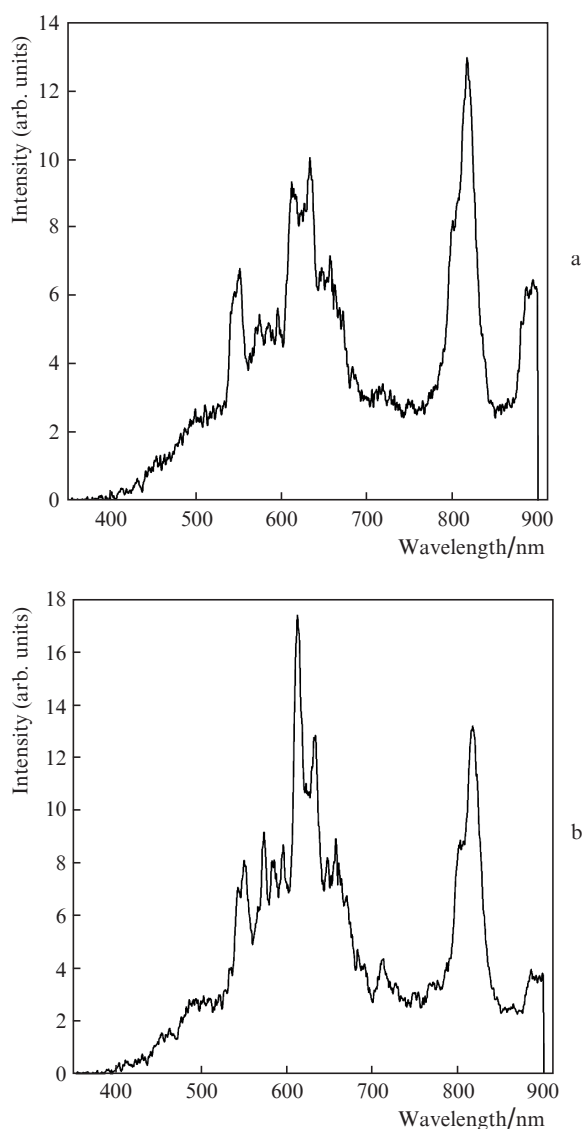


Figure 6. PCL spectra of undoped $(Y_2O_3)_{0.94}(ZrO_2)_{0.06}$ (a) and $(Y_2O_3)_{0.94}(HfO_2)_{0.06}$ (b) ceramics.

niium (hafnium) ions substituting the yttrium ions, the elementary cube can grow to the perfect $Zr(Hf)O_8$ cubes due to displacement of oxygen ions from neighbouring elementary cubes. As a result, a part of neighbouring cubes transforms into distorted tetrahedra. It is these tetrahedra in which Zr^{3+} (Hf^{3+}) ions may lie. The lowest level of these ions in the tetrahedral sites is the orbital doublet E, and the upper level is the triplet T_2 with an energy equal to the crystal field strength $10Dq$. The presence of two luminescence bands is explained by the existence of two types of tetrahedra, for example, with different distortion degrees. Taking into account the luminescence wavelengths, the orbital triplet energy is estimated to be approximately 12225 cm^{-1} in one of the tetrahedra and about 11100 cm^{-1} in the other. These energies are close to the energies of the ${}^4F_{5/2}$ ($12138\text{--}12436\text{ cm}^{-1}$) and ${}^4F_{3/2}$ ($11208\text{--}1404\text{ cm}^{-1}$) levels of the Nd^{3+} ion [28], and, hence, the Zr^{3+} (Hf^{3+}) impurity ions with these energies are good acceptors for neodymium ions.

For the upper ${}^2F_{5/2}$ level of Yb^{3+} with an energy of $10300\text{--}10700\text{ cm}^{-1}$ [28], the dipole–dipole interaction can occur only with a centre emitting at a wavelength in the region

of $\lambda \approx 900\text{ nm}$. Therefore, Yb^{3+} ions also must undergo the Förster quenching. This is evidenced by a noticeable decrease in the quantum yield of luminescence of Nd^{3+} ions with introduction of hafnium and zirconium. However, as is shown in [24, 27], the effective luminescence decay time of Yb^{3+} ions within the measurement error of $\pm 50\text{ }\mu\text{s}$ remains constant and coincides with the radiative lifetime of the upper laser level ${}^2F_{5/2}$ of the Yb^{3+} ion, $\tau_{\text{eff}} \approx \tau_r \approx 1200\text{ }\mu\text{s}$, independently of addition of zirconium or hafnium. However, this does not mean that the Förster quenching is absent in the studied ceramics. Indeed, as follows from (1), at $\tau_r > 4\tau_F$, the measured effective time τ_{eff} almost coincides with the radiative time τ_r . In this case, the Förster quenching time τ_F should be determined by direct approximation of the luminescence decay curve by formula (1).

4. Conclusions

A method of production of highly transparent ceramics with disordered crystal-field structure based on solid solutions of iso- and heterovalent elements in yttrium oxide is developed. These additives broaden the spectral bands of laser transitions of active neodymium and ytterbium ions. This is more pronounced in the case of introduction of heterovalent additives. Lasing was obtained in several ceramic samples.

We believe that an important reason for the relatively low lasing efficiency and the absence of lasing in the $[(Nd_{0.01}Y_{0.99})_2O_3]_{0.88}(ZrO_2)_{0.12}$ ceramic sample with the best transparency is the Förster quenching of the upper laser levels and pump levels. It is found that the characteristic time of the Förster quenching decreases with introduction of heterovalent additives. It is suggested that, in this case, in addition to the well-known mechanism of quenching on intrinsic defects—acceptors, there are quenching mechanisms in which the role of acceptors is played by impurity defects in the form of Zr^{3+} (Hf^{3+}) ions lying in distorted tetrahedra. It should be noted that the question of the nature of acceptors cannot yet be considered as solved. It is necessary to study how to optimise the concentration of heterovalent additives.

The synthesised ceramics based on solid solutions is a promising material for active laser media emitting ultrashort pulses.

Acknowledgements. We thank Yu.V. Orlovskii (A.M. Prokhorov General Physics Institute, Russian Academy of Sciences) for helpful discussions of this problem. The work was supported by the Programme ‘Extreme Light Fields and Their Applications’ of the Presidium of the Russian Academy of Sciences (No. 12-P-2-1011); by the Programmes of the Presidium of the Ural Branch of the Russian Academy of Sciences (Nos 12-2-002-YaTs and 12-2-003-YaTs); and by the Russian Foundation for Basic Research (Grant No. 11-08-0005a).

References

- Anderson R.C. US Patent № 3545987 (1970).
- Jorgensen P.J., Anderson R.C. *J. Am. Ceram. Soc.*, **50**, 553 (1967).
- Greskovich C., Woods R.N. *Am. Ceram. Soc. Bull.*, **52**, 473 (1973).
- Greskovich C., Chernoch J.P. *J. Appl. Phys.*, **44**, 4599 (1973).
- Greskovich C., Chernoch J.P. *J. Appl. Phys.*, **45**, 4495 (1974).
- Borovkova L.B., Lukin E.S., Poluboyarinov D.N. *Trudy MKhTI im. D.I. Mendeleeva*, **68**, 85 (1971).
- Lukin E.S., Glazychev V.S. *Steklo i Keramika*, **1**, 16 (1980).

8. Glazychev V.S., Lukin E.S., Borovkova L.B. *Ogneupory*, **3**, 44 (1978).
9. Glazychev V.S., Lukin E.S., Balashov V.A., Borovkova L.B. *Izv. Akad. Nauk SSSR. Ser. Neorg. Mater.*, **13**, 1814 (1977).
10. USSR Certificate of Authorship, No. 606305b, MKI³ SO4V 35/64.
11. Bakunov V.S., Belyakov A.V., Lukin E.S., Shayakhmetov U.Sh. *Oksidnaya keramika: spekanie i polzuchest'* (Oxide Ceramics: Sintering and Creep) (Moscow: RKhTU im. D.I. Mendeleeva, 2007).
12. Ikesue A., Kamata K., Yoshida K. *J. Am. Ceram. Soc.*, **79**, 359 (1997).
13. Hou X., Zhou S., Li Y., Li W. *Opt. Mater.*, **32**, 920 (2010).
14. Li W., Zhou S., Lin H., Teng H., Liu N., Li Y., Hou X., Jia T. *J. Am. Ceram. Soc.*, **93**, 3819 (2010).
15. Hou X., Zhou S., Jia T., Lin H., Teng H. *J. Lumin.*, **131**, 1953 (2011).
16. Sato Y., Saikawa J., Taira T., Ikesue A. *Opt. Mater.*, **29**, 1277 (2007).
17. Saikawa J., Sato Y., Taira T., Ikesue A. *Opt. Mater.*, **29**, 1283 (2007).
18. Kurokawa H., Shirakawa A., Tokurakawa M., Ueda K., Kuretake S., Tanaka N., Kintaka Y., Kageyama K., Takagi H., Kaminskii A.A. *Opt. Mater.*, **33**, 667 (2011).
19. Tokurakawa M., Shirakawa A., Ueda K., Yagi H., Yanagitani T., Kaminskii A.A. *Techn. Dig. Conf. on Lasers and Electro-Optics/ International Quantum Electronics* (Baltimore, Maryland, Optical Society of America, 2009) paper CFO3.
20. Tokurakawa M., Shirakawa A., Ueda K., Yagi H., Noriyuki M., Yanagitani T., Kaminskii A.A. *Opt. Express*, **17**, 3353 (2009).
21. Osipov V.V., Khasanov O.L., Solomonov V.I., Shitov V.A., Orlov A.N., Platonov V.V., Spirina A.V., Luk'yashin K.E., Dvilis E.S. *Izv. Vuzov, Ser. Fiz.*, **53**, 48 (2010).
22. Osipov V.V., Kotov Yu.A., Ivanov M.G., Samatov O.M., Lisenkov V.V., Platonov V.V., Murzakaev A.M., Medvedev A.I., Azarkevich E.I. *Laser Phys.*, **16**, 116 (2006).
23. Khasanov O., Osipov V., Dvilis E., Kachaev A., Khasanov A., Shitov V. *J. Alloys Compd.*, **509**, S338 (2011).
24. Osipov V.V., Solomonov V.I., Shitov V.A., Maksimov R.N., et al. *Opt. Atmos. Okean.*, **25**, 207 (2012).
25. Bagaev S.N., Osipov V.V., Ivanov M.G., Solomonov V.I., Platonov V.V., Orlov A.N., Rasulaeva A.V., Ivanov V.V., Kaigorodov A.S., Khrustov V.R., Vatnik S.M., Vedin I.A., Maiorov A.P., Pestryakov E.V., Shestakov A.V., Salkov A.V. *Kvantovaya Elektron.*, **38** (9), 840 (2008) [*Quantum Electron.*, **38** (9), 840 (2008)].
26. Bagayev S.N., Osipov V.V., Ivanov M.G., Solomonov V.I., Platonov V.V., Orlov A.N., Rasuleva A.V., Vatnik S.M. *Opt. Mater.*, **31**, 740 (2009).
27. Bagayev S.N., Osipov V.V., Shitov V.A., Pestryakov E.V., Kijko V.S., Maksimov R.N., Lukyashin K.E., Orlov A.N., Polyakov K.V., Petrov V.V. *J. Eur. Ceram. Soc.*, **32**, 4257 (2012).
28. Kaminskii A.A. *Lazernye kristally* (Laser Crystals) (Moscow: Nauka, 1975).
29. Kumar G.A., Lu J., Kaminskii A.A., Ueda K., Yagi H., Yanagitani T. *IEEE J. Quantum Electron.*, **42**, 643 (2006).
30. Osipov V.V., Rasulaeva A.V., Solomonov V.I. *Opt. Spekr.*, **105**, 591 (2008).
31. Schaack G., Koningstein J.A. *J. Opt. Soc. Am. A*, **60**, 1110 (1970).